A New Approach for Stress State - Dependent Flow Localization Failure Bounded Through Ductile Damage in Dynamically Loaded Sheets

F. Hosseini Mansoub [1], A. Basti [2,*] , A. Darvizeh [2], A. Zajkani [3]

[1]*Department of Mechanical Engineering, University Campus, University of Guilan, Rasht, Iran*
[2]*Department of Mechanical Engineering, University of Guilan, Rasht, Iran*
[3]*Department of Mechanical Engineering, Imam Khomeini International University, Qazvin, Iran*

ABSTRACT

In this paper, a new approach is proposed for stress state - dependent flow localization in bifurcation failure model bounded through ductile damage in dynamically loaded sheets. Onset of localized necking is considered in phenomenological way for different strain rates to draw the forming limit diagram (FLD). Using a strain metal hardening exponent in the Vertex theory related to the strain rate helps investigate rate-dependent metal forming limits. Besides, the paper utilizes the model of ductile damage as a function of strain condition, stress states (triaxiality and Lode parameters), and the symbols of stiffness strain to predict the onset of the necking. It is worth noting that updated level of elasticity modulus in the plastic deforming is attributed as an essential index for the ductile damage measuring. According to original formulations, a UMAT subroutine is developed in the finite element simulation by ABAQUS code to analyze and connect the related constitutive models. Results reveal that the FLD levels increase for St 13 material through enhancing the strain rate.

© 2020 IAU, Arak Branch. All rights reserved.

Keywords: Ductile damage; Stress state; Strain rate; Forming Limit; Localized necking.

1 INTRODUCTION

INVESTIGATING sheet metal formability to avoid defected parts and optimize their operation is of extreme importance. The level of deformation in the process of sheet metal forming is limited with necking, shrinkage or rupture. This investigation on sheet metal formability could also be titled as obtaining the limit of sheet metal tolerance. In recent years, numerical simulations have gained further significance in different industries like aerospace and automotive. Numerical simulation is an efficient way to expand industrial cycle by reducing high experimental costs in their various aspects such as fracture, failure, etc. Considering the importance of the fracture

_____

[*]Corresponding author. Tel.: +98 133 3690033; Fax: +98 133 3461551.
E-mail address: basti@guilan.ac.ir (A. Basti).

phenomenon in different industrial applications, a proper understanding of its concept and modeling in numerical simulations is of vital significance for official predictions. Furthermore, the importance of predicting damage in various fields of industry has increased. However, damage phenomenon has been investigated from multiple points of view, and numerous models have been proposed for material damage. Another purpose the present study aims to serve is to analyze formability limit of sheet metals based on ductile damage criterion dependent on strain condition and on hydrostatic pressure and the Lode parameter as well. Various geometries are used to create different strain conditions for different shapes of parts loadings. The finite element analysis (FEA) has been recently used extensively to collect the data required for a real process of forming in the industry. In this method, data on deforming, distribution of stress and strain, punch force and fracture are acquired. Moreover, using criteria of ductile fracture in recent years has gained popularity in predicting FLDs. In 1999, Takoda et al. [1] used a ductile fracture criteria named as Cockroft, Brozzo, and Clift along by the finite element method to predict the FLD for some types of steel and alloys of aluminum. They compared their findings with empirical results and demonstrated that the FLD could be easily predicted via ductile fracture criteria. Faguo Li et al. [2] examined the FLD for St 14 based on ductile fracture criteria as their findings precisely confirmed results from laboratory experiments. The first model of localized necking was proposed by Hill [3]. This model treats localized necking as a kind of material instability assuming that localized band forms along the zero-extension direction. An extension of Hill's model is the theory of acoustic tensor [4], which has been further investigated by later scholars. One of the drawbacks of the acoustic tensor theory is that it could only be applied to localized necking of strain-softening materials, such as hot metals, solder, rocks, etc. [5–12]. Marciniak and Kuczynski developed the second model of localized necking as called the M–K model [13]. This model is a significant physically approach with pure mathematics. Therefore, it is widely employed by practicing engineers. However, researchers have found that M–K model is too sensitive to the size and the depth of the original band required to fit the theoretical predictions to the experimental data [14, 15]. Recently, Hashemi et al studied the effects of normal and through-thickness shear (TTS) stresses were simultaneously considered to predict the generalized forming limit diagram (GFLD) of AA3104-H19 using Yld96, Yld2004 and Yld2011 anisotropic yield criteria. For this purpose, considering the general stress state, including the normal and through-thickness shear stresses, the modified Marciniak–Kuczynski (M–K) model was employed. The results show that the through-thickness shear stress has positive sensitivity on the limit strains. Also, the normal stress is more efficient than the through-thickness shear stress on the formability of the plate. Comparison between the results indicates that the predicted limit strains by the Yld2011 anisotropic yield function are lower than those predicted by Yld96 [16]. As well as they studied The substitute presentations of the conventional forming limit diagram (FLD) are stress-based forming limit diagram (FLSD), extended stress forming limit diagram (XSFLD), and polar effective plastic strain forming limit diagram (PEPS-FLD). These diagrams have already been proposed as alternative criteria to the conventional FLD for predicting forming limits in processes that sheet does not experience proportional or in-plane loading conditions. The present study provides a complete comparison of different forms of forming limit diagrams. For this purpose, FLD and extended FLDs are predicted based on the modified Marciniak and Kuczynski (M-K) model with Yld2011 anisotropic yield function while various factors that cause a change in the FLD of a specific alloy including initial imperfection coefficient, non-linear strain path, through-thickness normal and shear stresses are considered. The results indicate that all forms of extended diagrams are independent of strain path and the diagrams in stress space (i.e., FLSD and XSFLD) are less sensitive to the strain path than PEPS-FLD. In this regard, the main weakness of XSFLD, especially on the right-hand side, is that the safety margin cannot be visualized easily. By increasing the initial imperfection coefficient, the level of all forms of diagram increases. However, the effect of through thickness stresses on different diagrams is not the same. Increase in normal and shear stresses results in a downward shift in FLSD and an upward shift in other types of forming limit diagrams [17]. The Vertex theory is a basis for localized necking develops eventually on a yield surface under a loading path [18, 19]. The direction of plastic flow at the Vertex shows uncertainty, which triggers inhomogeneous deforming. In other words, localized band forms on the sheet metal. All over the localized band, plastic strain rate demonstrates discontinuity. This is a phenomenon of material bifurcation. Later on, the Vertex theory was redeveloped to produce a more comprehensible mathematical form, which enables the implementation of advanced constitutive relations based on a high-order yield criterion coupled with an anisotropic damage model [20]. Recently, Zajkani et al. [18] studied a diffuse to localized necking transition in rate-dependent bifurcation analysis based on the Vertex model. Moreover, they introduced substantial discussions around this model involving path-dependent instability for the substrate - supported composite plates [19, 21]. Wierzbicki et al. successfully modeled a fracture for the static loading with continuous damage. The significance of their study was in the features of damage development rule covering strain development, the fracture dependent on hydrostatic pressure and the Lode angle [22, 23]. Hari Manoj Simha et al. modified Xue-Wierzbicki model of damage mechanism [22] so that it included strain rate and utilized it for modeling dynamic response and fracture in X70 steel pipe in the drop weight tear test. The development of

damage was dependent on Lode angle, hydrostatic pressure and strain rate [24]. Campos et al. [25] studied the FLD of stainless steel AISI304 both empirically and numerically and demonstrated that the FLD of aluminum depends slightly on strain rate. Kim et al. [26] probed the effect of strain rate on CQ steel's forming limit criterion, conducted tests on different directions to the rolling and proved that this material is dependent on strain rate. Measurement of directional anisotropy coefficients and prediction of forming limit curve were done by Hashemi et al. [27] Furthermore, in studies on the effect of strain rate on ductile damage, plasticity models had to be considered so that they depend on strain rate. [28]. The plasticity model based on strain rate and temperature placed in the mechanical framework of continuum damage was utilized by Brunig and Gerke [29, 30]. The effect of strain rate on plastic anisotropy of advanced high strength steel sheets was studied by Huh et al. [31]. The experiments they conducted on strain rates over 100/s on TRIP590 and DP780 steels ended in plastic anisotropy while increasing strain rate. Unlike the models mentioned above, Johnson-Cook (J-C) model with its high popularity does not have any physical basis and is thoroughly experimental [32]. This multiplicative analysis model of flow strain assumes three functions dependent on the strain, strain rate, and temperature. Several studies on collision engineering have demonstrated that simple J-C plastic model offers acceptable predictions from the visco-plastic response dependent on temperature in metals under large strains [33–37]. Under static and isothermal loading conditions, the J-C model is reduced to exponent model used mainly in automotive industries to estimate stiffness strains of steels [38]. The effect of stress state on the ductile fracture has also been widely investigated in low strain rates in high-resistance steels [39–43]. Huh, et al. used a fast hydraulic test machine to conduct unidirectional tensile tests on four high resistance sheets of steel for the pre-necking state in strain rates ranging from 0.003/s to 200/s. They reported fracture elongation for TRIP600 steel and on elongation insensitive to rate for three other steel sheets [44]. On the other hand, Curtze et al. conducted static tensile tests with an average strain rate by using a hydraulic machine as well as high strain rate tests using Hopkinson's bar tensile system at room temperature. However, fracture elongation of DP600 steel without considering strain rate was almost as the same of TRIP700 steel. [45]. However, in all cases, prediction of necking to failure in the tensile test with a high strain rate is negligible; yet, strain fracture has not determined the necking position inside. Estimating local strain is also available in the onset of fracture at the tests with high strain rate for balk materials. Results from dynamic tests on the tension of symmetric parts with bands are the basis for the formulation of the J-C empirical model. On the other hand, according to the J-C model, ductility is introduced as a function of strain rate for copper, iron, and steel 4330 increases [32]. The positive sensitivity of the strain in the fracture to strain rate was determined through static and dynamic tests of tension in banded parts of aluminum 5083 [33] and steel FV535 [34]. Mohr and Roth conducted tests on flat parts with the central hole and various bands at low, average and high strain rates. They utilized J-C model coupled with Voce-swift stiffness strain compound function and the anisotropic flow rule to elaborate on post-necking states of parts. Fracture strain inside necking region was determined via finite element analysis and the combination of correctors obtained from high-speed photography. Loading routes to the onset of fracture in the tests were identified to indicate stress triaxiality, Lode angle parameter, temperature, strain rate and equivalent plastic strain [46]. Nevertheless, using J-C model demonstrates severe limitations when an accurate description of stiffening in the considerable strain is needed. One outstanding example of predicting necking response and post-necking is the sheet metals. Recently, several factors on prediction of forming limit curves (FLC) were studied by Hashemi et al. They analysis of aluminum alloy considering the through-thickness normal stress, anisotropic yield functions and strain rate. They found that the anisotropic plastic behavior and FLC of AA3104-H19 predicted by Yld2011 yield criterion are in good agreement with experimental data and are more accurate than those of Karafillis–Boyce (K–B) and Yld96 yield functions. In addition, according to FLD, the formability of sheet metal increases by applying the through-thickness normal stress. The effects of strain rate at quasi-static condition and temperature are theoretically investigated on the FLD of AA3104 aluminum alloy. The positive temperature sensitivity and negative strain rate sensitivity are observed of FLD of AA3104 [47].

The present paper gives an efficient method based on the Vertex theory in localized necking in order to determine FLDs, including strain rate dependences. Besides, introducing an accurate damage function based on simple continuum damage mechanics (CDM), the model is related to the stress state (Triaxiality and Lode parameters). The model will determine an element when it has reached the critical point of the failure. According to the principle of the CDM, the elastic modulus will be decreased as a characterization parameter during plastic deformation. It is inserted in the model through a new normalized ductile damage criterion. In the application of the ABAQUS for a finite element simulation, a UMAT subroutine is established for computation of major and minor strain, considering above concepts which enable the model to evaluate the initiation of instability and obtain the FLDs, phenomenologically. A typical strain-rate-dependent metal, St 13, is chosen for validation of the modified Vertex theory. To examine the accuracy of the results from the present simulation and compare with the experimental results, applicability is considered. Forming limit tests are also performed for St 13 sheets to measure

the FLD. It is worthy to mention that all these concerns have not been considered simultaneously in the previous studies.

2   DUCTILE DAMAGE CONTROLLER MODEL

Plastic deforming is the process of accumulation of damage. Nevertheless, a crack does not occur unless the value of damage variable reaches a critical point. The elasticity modulus will decrease the plastic deforming and this will be due to the accumulation of damage in the material. Damage accumulation decreases effective bearing area and the present elasticity modulus E_D in deformable materials. The damage performance is predicted for metal materials via elasticity modulus E_D ₑw be ca which expressed as follow:

$$E_D = E_0 e^{-p\varepsilon} \tag{1}$$

$$D = 1 - \frac{E_D}{E_0} = 1 - e^{-p\varepsilon} = \frac{A_0 - A_D}{A_0} \tag{2}$$

where:
   D Damage variable.
   A_0 Initial cross-sectional area of the gauge section.
   A_D Cross-sectional area after deforming damage.
   E_0 Initial Young's modulus   of virgin material.
   E_D Young's modulus   after deforming damage.
   ε True strain
   The damage function R is defined as follows:

$$R = \frac{D_i}{D_c} \tag{3}$$

The value of R is determined between zero (undamaged) and one (fracture). D_c is the critical value of the ductile damage. D_c in the uniaxial tension stress state can be obtained by:

$$D_c = f\left(\eta,\bar{\theta}\right)\left(1 - e^{-p\varepsilon_f}\right) \tag{4}$$

where η is the triaxiality and $\bar{\theta}$ is the Lode angle. Also, ε_f is the fracture strain calculated through $\varepsilon_f = n^p e^{(p/2)}$ as $p = 1$ and $p = 9(1-v)/4$ represent a true and nominal fracture strains, respectively. The value of p is relevant to the strain-hardening exponent in plastic deforming of materials: $f\left(\eta,\bar{\theta}\right)$ is the function of stress state parameters and can be expressed according to reference [2] as:

$$f\left(\eta,\bar{\theta}\right) = 0.558\sinh\left(1.5\eta\right) - 0.008\bar{\theta}\cosh\left(1.5\eta\right) \tag{5}$$

To calculate this function, the process of the finite element analysis could be adopted with incremental formulas as the expression of damage accumulation

$$\Delta D_i = f_i\left(\eta,\bar{\theta}\right)pe^{-p\varepsilon_i}\Delta\varepsilon_i \tag{6}$$

$$D_i = D_i + \Delta D_i \tag{7}$$

Above equations, when $D_i \leq 0$ the value is considered equal to zero. The damage variable value R can be acquired through Eq. (3). Therefore, $R = 0$ means that no damage has occurred in materials or the original damage has been repaired yet. The damage emerges in the material when $0 \prec R \prec 1$, and the plastic deforming could be continued. However, the materials reach the limit of deforming damage $R = 1$, where the ductile fracture begins. All equations are compiled through a User-defined material subroutine as exported to Abaqus package for the mechanical behavior. So that it is convenient for us to apply this damage criterion to other materials.

3   VERTEX LOCALIZED PREDICTOR MODEL

As it could be seen in Fig.1, a localized necking band appears on the surface of the sheet under a critical condition on a sheet metal under in-plane stretch. σ_1 and σ_2 in this figure are principal stresses. The principal strains along with the σ_1 and σ_2 directions are known as major strain ε_1 and minor strain ε_2. In fact, forming limit strains are the major and minor strains at the critical state of localized necking.

According to the Vertex theory, a localized necking band appears at the same time when Vertex appears on the yield surface. The velocity discontinuity between inside and outside of the localized band is:

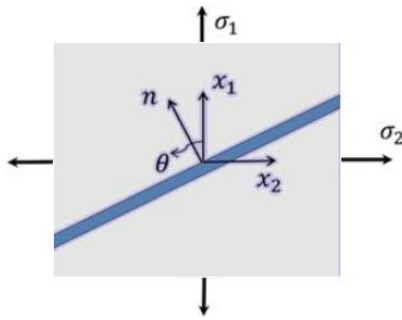$$\Delta v_i = v_{i,inside} - v_{i,outside} = f_i(n,x) = f_i(n_k x_k) \qquad (i,k = 1,2) \tag{8}$$

Fig.1
The Vertex model with the localized necking band.

In this equation, n_k, $(k = 1,2)$ are the components of normal vector n. When we have $n_1 = \cos\theta$ and $n_2 = \sin\theta$, the discontinuity of deforming gradient rate is:

$$\Delta\left(\frac{\partial v_i}{\partial x_j}\right) = \frac{\partial(\Delta v_i)}{\partial x_j} = g_i n_j \qquad (i,j = 1,2) \tag{9}$$

Within the localized band, g_i $(i = 1,2)$ is non- zero. It also varies along the normal direction. Since the strain rate is $\dot{\varepsilon}_{ij} = (\partial v_i / \partial x_j)$, we can write the principal strain-rate discontinuity across the localized band as:

$$\Delta\dot{\varepsilon}_1 = g_1 n_1 \qquad \Delta\dot{\varepsilon}_2 = g_2 n_2 \tag{10}$$

After localized necking appears in the homogeneous region, the one and two directions remain. There is, however, no guarantee inside the necking for the main directions to stay that way. In other words, at some point, inside the necking, $\sigma_{12} = 0$ may not be true anymore. According to the studies conducted by Jie et al. [48] on the limit strain based on the Vertex theory and considering the strain exponent equation, the equivalent strain and the strain rate as $\bar{\sigma} = K\bar{\varepsilon}^n\bar{\varepsilon}^m$ will give:
On the left side of the FLD curve:

$$\varepsilon_1 = \frac{m+n}{1+\beta} + \frac{\sqrt{3}(m+n)s(\bar{\sigma},\bar{\varepsilon})}{2\sqrt{1+\beta+\beta^2}} \qquad (11)$$

On the right side of the FLD curve:

$$\varepsilon_1 = \frac{3\beta^2 + (m+n)(2+\beta)^2}{2(2+\beta)(1+\beta+\beta^2)} + \frac{(m+n)s(\bar{\sigma},\bar{\varepsilon})}{2(2+\beta)\sqrt{1+\beta+\beta^2}} \times \left((2+\beta)\sqrt{3(1+\beta+\beta^2)}\bar{\varepsilon} - 3\beta^2 \right) \qquad (12)$$

The Vertex theory employs a deforming theory of plasticity. Here, we apply the J_2 deforming theory based on the Von Mises yield criterion. Where n is the stiffness strain value, m is the exponent of sensitivity to strain rate, and k is the stiffness coefficient calculated via uniaxial tests. β is the ratio of minor strain to major strain during the loading process and $s(\bar{\sigma},\bar{\varepsilon}) = -c\bar{\sigma}/\bar{\varepsilon}^{\frac{n}{m+1}}$ in which $\bar{\varepsilon}$ and $\bar{\sigma}$ are an equivalent strain, equivalent stress of the Von Mises and c is an integration constant, which can be determined from the uniaxial test at various strain rates. These values reveal final strain for sheet metals relevant to strain rate and considering localized necking based on the Vertex theory.

The process of calculation and judgment in sheet's plastic deforming has been plotted in Fig.2.
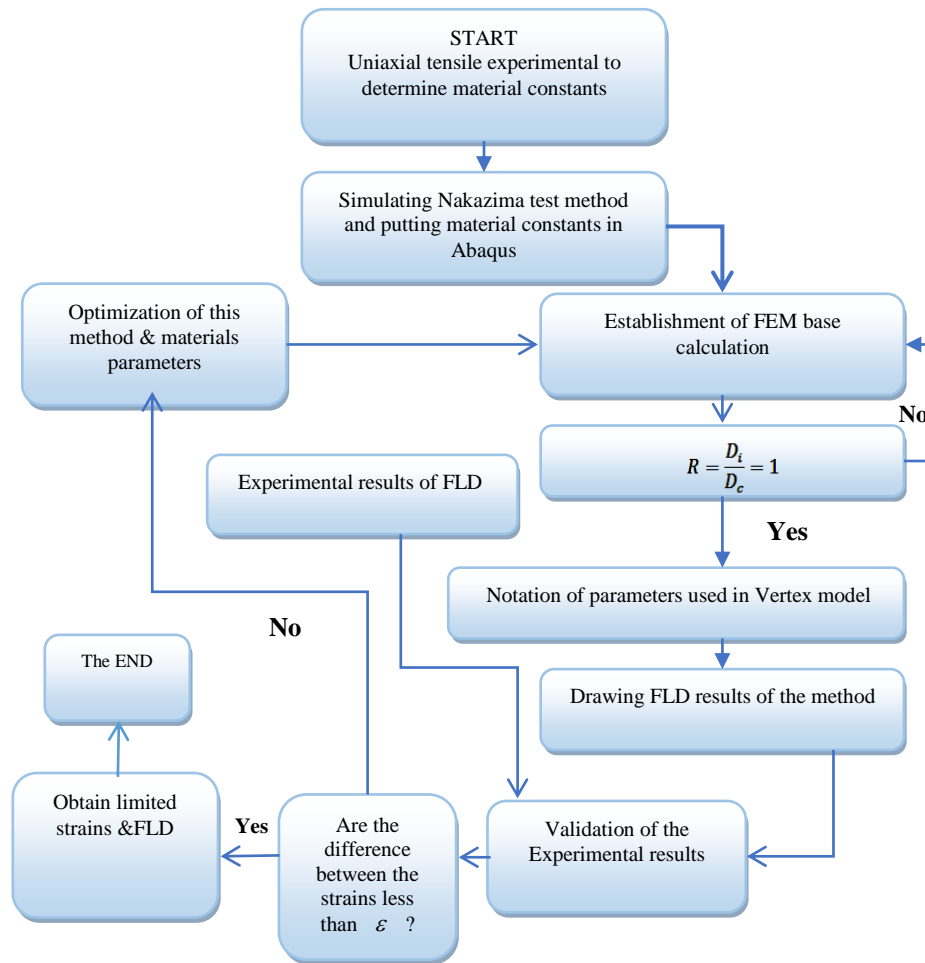

Fig.2
The process of calculation and judgment in sheet's plastic deforming.

4   NUMERICAL MODEL IN ABAQUS APPLICATION

All the specimens in Fig.3 (based on the standard of ASTM E2218) were simulated using commercially available finite element code ABAQUS/Explicit.
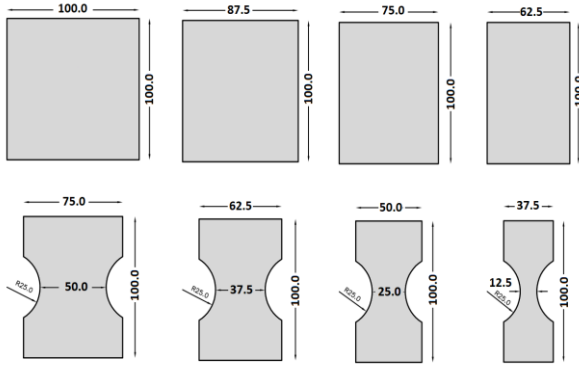

Fig.3
Different specimen geometry of the hemispherical dome stretching test.

To simulate the drawing process, the sheet is considered the formable while other parts are regarded as the solid. Physical properties like density, elastic properties like Young's modulus and Poisson's ratio, plastic properties and damage criteria are all put into the application in the form of data. These requirements include the formability limit of St13 and St14 steel dependent on strain rate and the dynamic formability diagram. Moreover, the mechanical properties of these materials are represented in Table 1.

Table 1
The mechanical and constants values properties of St 13 and St14 steel sheets [2, 48, 49].

Materials	Elasticity modulus (GPa)	Density (g/mm³)	Yield stress (MPa)	ϑ	m	n	k (MPa)	c (MPa⁻²)
St13	180	7.85	250	0.3	0.0191	0.2387	650	-5×10^{-5}
St14	210	7.85	300	0.3	0.0187	0.23	524.58	-5×10^{-5}

It is, however, worth mentioning that, according to Eq. (5), the critical damage values are calculated to be 0.1387 and 0.1374 for ST13 and St14 respectively. Furthermore, the contact state between the sheet and the holder, sheet, and mandrel and sheet and the matrix are defined as a simple contact. The friction coefficient between sheet, holder, and matrix and between sheet and mandrel was considered 0.2 and 0.12 respectively.

The sheet is divided into meshes with R3D4 and C3D8R elements. To decrease analysis time due to symmetry and similarity of a quarter of the specimen is modeled and the factor 1000 is selected for the mass scaling option. Sizes of the meshes are considered 1 *mm*, and the thickness of the sheet is also 1 *mm*. It is suggested that the minimum length of element should be higher than the shell thickness, based on the mesh sensitivity study [2]. Forming limit criterion must be solved gradually for the damage and plasticity have non-linear behavior. In each stage, data from the earlier stage of strain development put into a subroutine, and the strain, damage, plastic strain and major strains along with minor strains are calculated as the output. Moreover, the behavior of materials is modeled elastically and plastically where the plasticity were modeled as anisotropic and isotropic, while the elasticity considered to be isotropic. What is more, the constitutive relation, yield criteria and ductile damage criteria of this material were compiled in user material subroutine (UMAT) of ABAQUS. And according to the formulations proposed above, the UMAT subroutine in the finite element application of the ABAQUS is used to analyze the model, including 10 variables. For instance, SDV1 and SDV4 are defined as the plastic strain and damage value respectively. All variables can affect the definition of the damage value. When the damage value reaches the unit, the analysis stops until each element with its damage value reaches the critical point. In this state, the SDV4 reaches unit Fig.4 and other parameters like the plastic strain, Von Mises stress and the strain rate are noted and picked up to input into the Vertex equations to draw the forming limit diagrams. In this method, we were able to control the required parameters of the Vertex model as equivalent stress and equivalent plastic strain by damage function. Then they are classified based on strain rate to obtain FLDs in distinctive strain rate. It is noticeable to achieve different strain rates on the elements; loading rate is changed.

5   RESULTS AND DISCUSSION

Here are some of the responses received from analysis of the specimen. After finishing models with different dimensions and shapes under various strain rates, their FLDs and the effect of strain rate on diagrams were investigated.
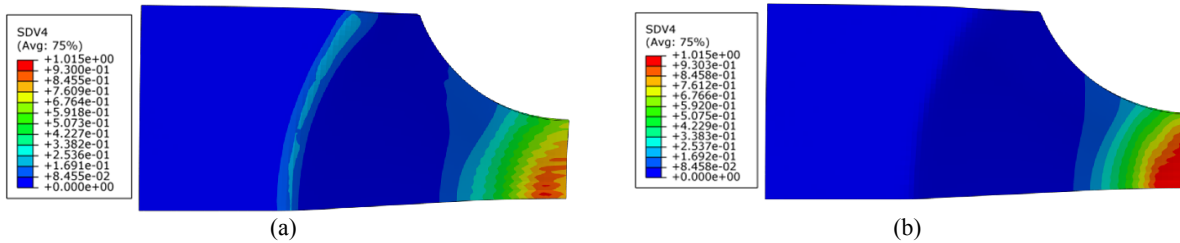

(a)   (b)

Fig.4
The contours of the damage value in loading velocity: a) 100 *m/s*   b) 1 *m/s*. for St 13.

There is a relationship between formation of sheet metals, creation of instabilities, their accumulation and their fracture with stress, strain, yield stress, stiffness, and instability. The yield criterion and stiffness rule determine the level of the formability of sheet metals referring to various loading states. In other words, instability criterion reveals when strain and stress will induce instability. This strain is considered to be the ultimate strain in this paper. This theory is the determining factor in the confining state of sheet metal formability calculated earlier in the present paper. The present paper can give a method to determine the FLDs by which the Vertex theory is used to enter strain rates into calculations. Moreover, introducing damage function will determine an element that has reached the critical point and failure has occurred in it. However, not all these criteria have been considered in a single study altogether. To examine the accuracy of the results from the present study and compare them with the experiments conducted by previous scholars, applicability in two states is considered. One is dependent on the strain rate (strain rate 20 1/*s*), and the other is independent on strain rate (considering *m* = 0 in power hardening function). The comparisons for st13 and st14 materials are seen in Fig.5.
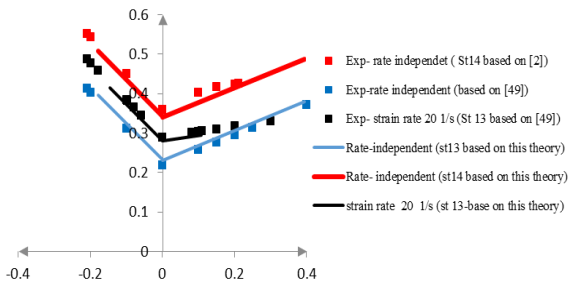

Fig.5
Validation and comparison of the presented results of this theory with the experimental results for the St 14 [2] and M-K model [49].
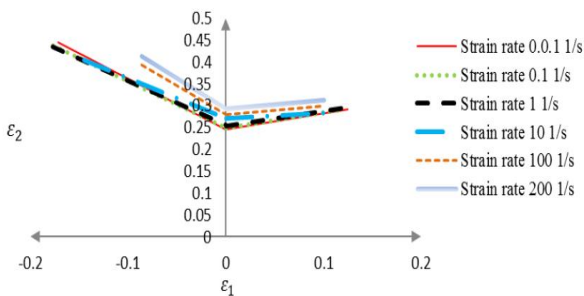

Fig.6
Forming limit diagram of St13 in various strain rates and their comparison.

The level of forming limit diagrams goes up as strain rate increases; yet, this effect is negligible in low (static) strain rates and is more observed in higher strain rates in the FLDs. Fig.6. These findings concur with findings other scholars calculated and reached through other methods [34, 49–52].

6   CONCLUSION

This paper gives an efficient method based on Vertex theory to determine the FLDs, including strain rate calculations. Besides, introducing a damage function based on a simple continuum damage mechanics (CDM) is dependent on the stress state (Triaxiality and Lode parameters). Considering above concepts, which enable the model to evaluate the initiation of the instability and obtain the FLDs, phenomenologically in the application of the ABAQUS for a finite element simulation, a UMAT subroutine is established for major and minor strain. The model will determine an element when it has reached the critical point of the failure. When the damage value reaches the unit, the analysis stops until each component with its damage value reaches the critical point. In this state, other parameters like the major strain, minor strain, Von Mises stress and the strain rate are noted and picked up to input into the Vertex equations to draw forming limit diagrams and then classifying them based on strain rate to obtain FLDs in distinctive strain rate.

It is worthy to mention that all these concerns have not been considered simultaneously in previous studies. As it can be seen in the results, effects of strain rate on the level of FLDs goes up as strain rate increases; yet, this effect is negligible in low (static) strain rates and is more observed in higher strain rates in the FLDs. These findings concur with findings other scholars calculated and reached through different methods.

REFERENCES

[1]   Aboutalebi F.H., Farzin M., Poursina M., 2011, Numerical simulation and experimental validation of a ductile damage model for DIN 1623 St14 steel, *The International Journal of Advanced Manufacturing Technology* **53**: 157-165.

[2]   Ma X., Li F., Li J., 2015, Analysis of forming limits based on a new ductile damage criterion in St14 steel sheets, *Materials & Design* **68**: 134-145.

[3]   Hill R., 1952, On discontinuous plastic states, with special reference to localized necking in thin sheets, *Journal of the Mechanics and Physics of Solids* **1**:19-30.

[4]   Hill R., 1958, A general theory of uniqueness and stability in elastic-plastic solids, *Journal of the Mechanics and Physics of Solids* **6**: 236-249.

[5]   Borré G., Maier G., 1989, On linear versus nonlinear flow rules in strain localization analysis, *Meccanica* **24**: 36-41.

[6]   Thomas W.M., 1991, Friction stir butt welding, International Patent Application No PCT/GB92/0220.

[7]   Chow C.L., Jie M., Wu X., 2005, Localized necking criterion for strain-softening materials, *Journal of Engineering Materials and Technology* **127**: 273-278.

[8]   Neilsen M.K., Schreyer H.L., 1993, Bifurcations in elastic-plastic materials, *International Journal of Solids and Structures* **30**: 521-544.

[9]   Chow C.L., Jie M., Wu X., 2007, A damage-coupled criterion of localized necking based on acoustic tensor, *International Journal of Damage Mechanics* **16**: 265-281.

[10]   Szabó L., 2000, Comments on loss of strong ellipticity in elastoplasticity, *International Journal of Solids and Structures* **37**: 3775-3806.

[11]   Bigoni D., Hueckel T., 1991, Uniqueness and localization—I. Associative and non-associative elastoplasticity, *International Journal of Solids and Structures* **28**: 197-213.

[12]   Rudnicki J.W., Rice J.R., 1975, Condition for the localization of deformation in pressure-sensitive dilatant materials, *Journal of the Mechanics and Physics of Solids* **23**(6): 371-394.

[13]   Xue L., Wierzbicki T., 2008, Ductile fracture initiation and propagation modeling using damage plasticity theory, *Engineering Fracture Mechanics* **75**: 3276-3293.

[14]   Marciniak Z., Kuczyński K., 1967, Limit strains in the processes of stretch-forming sheet metal, *International Journal of Mechanical Sciences* **9**(9): 609-612.

[15]   Marciniak Z., Kuczyński K., Pokora T., 1973, Influence of the plastic properties of a material on the forming limit diagram for sheet metal in tension, *International Journal of Mechanical Sciences* **15**: 789-800.

[16]   Mirfalah S.M., Basti A., Hashemi R., Darvizeh A., 2018, Effects of normal and through-thickness shear stresses on the forming limit curves of AA3104-H19 using advanced yield criteria, *International Journal of Mechanical Sciences* **137**: 15-23.

[17]   Erfanian M., Hashemi R., 2018, A comparative study of the extended forming limit diagrams considering strain path, through-thickness normal and shear stress, *International Journal of Mechanical Sciences* **148**: 316-326.

[18]   Zajkani A., Bandizaki A., 2017, An efficient model for diffuse to localized necking transition in rate-dependent bifurcation analysis of metallic sheets, *International Journal of Mechanical Sciences* **133**: 794-803.

[19]   Zajkani A., Bandizaki A., 2017, A path-dependent necking instability analysis of the thin substrate composite plates considering nonlinear reinforced layer effects, *The International Journal of Advanced Manufacturing Technology* **95**: 759-774.

[20] Stören S., Rice J.R., 1975, Localized necking in thin sheets, *Journal of the Mechanics and Physics of Solids* **23**: 421-441.

[21] Zajkani A., Bandizaki A., 2018, Stability and instability analysis of the substrate supported panels in the forming process based on perturbation growth and bifurcation threshold models, *Journal of Manufacturing Processes* **31**: 703-711.

[22] Xue L., 2007, *Ductile Fracture modeling-Theory, Experimental Investigation and Numerical Verification*, Thesis Ph. D., Massachusetts Institute of Technology.

[23] Bai Y., Wierzbicki T., 2008, A new model of metal plasticity and fracture with pressure and Lode dependence, *International Journal of Plasticity* **24**: 1071-1096.

[24] Simha C.H.M., Xu S., Tyson W.R., 2014, Non-local phenomenological damage-mechanics-based modeling of the Drop-Weight Tear Test, *Engineering Fracture Mechanics* **118**: 66-82.

[25] Campos H.B., Butuc M.C., Grácio J.J., 2006, Theorical and experimental determination of the forming limit diagram for the AISI 304 stainless steel, *Journal of Materials Processing Technology* **179**: 56-60.

[26] Kim S.B., Huh H., Bok H.H., Moon M.B., 2011, Forming limit diagram of auto-body steel sheets for high-speed sheet metal forming, *Journal of Materials Processing Technology* **211**: 851-862.

[27] Mosavi F., Hashemi R., Madoliat R., 2018, Measurement of directional anisotropy coefficients for AA7020-T6 tubes and prediction of forming limit curve, *International Journal of Advanced Manufacturing Technology* **96**: 1015-1023.

[28] Balasubramanian S., Anand L., 2002, Elasto-viscoplastic constitutive equations for polycrystalline fcc materials at low homologous temperatures, *Journal of the Mechanics and Physics of Solids* **50**: 101-126.

[29] Brünig M., Gerke S., 2011, Simulation of damage evolution in ductile metals undergoing dynamic loading conditions, *International Journal of Plasticity* **27**: 1598-1617.

[30] Shojaei A., Voyiadjis G.Z., Tan P.J., 2013, Viscoplastic constitutive theory for brittle to ductile damage in polycrystalline materials under dynamic loading, *International Journal of Plasticity* **48**: 125-151.

[31] Huh J., Huh H., Lee C.S., 2013, Effect of strain rate on plastic anisotropy of advanced high strength steel sheets, *International Journal of Plasticity* **44**: 23-46.

[32] Johnson G.R., Cook W.H., 1983, A constitutive model and data for metals subjected to large strains, high strain rates and high temperatures, *7th International Symposium on Ballistics*, The Hague.

[33] Clausen A.H., Børvik T., Hopperstad O.S., Benallal A., 2004, Flow and fracture characteristics of aluminium alloy AA5083–H116 as function of strain rate, temperature and triaxiality, *Materials Science and Engineering* **364**: 260-272.

[34] Erice B., Gálvez F., Cendón D.A., Sánchez-Gálvez V., 2012, Flow and fracture behaviour of FV535 steel at different triaxialities, strain rates and temperatures, *Engineering Fracture Mechanics* **79**: 1-17.

[35] Kajberg J., Sundin K-G., 2013, Material characterisation using high-temperature Split Hopkinson pressure bar, *Journal of Materials Processing Technology* **213**: 522-531.

[36] Smerd R., Winkler S., Salisbury C., 2005, High strain rate tensile testing of automotive aluminum alloy sheet, *International Journal of Impact Engineering* **32**: 541-560.

[37] Verleysen P., Peirs J., Van Slycken J., 2011, Effect of strain rate on the forming behaviour of sheet metals, *Journal of Materials Processing Technology* **211**:1457-1464.

[38] Mohr D., Dunand M., Kim K-H., 2010, Evaluation of associated and non-associated quadratic plasticity models for advanced high strength steel sheets under multi-axial loading, *International Journal of Plasticity* **26**: 939-956.

[39] Kim J.H., Sung J.H., Piao K., Wagoner R.H., 2011, The shear fracture of dual-phase steel, *International Journal of Plasticity* **27**: 1658-1676.

[40] Lou Y., Yoon J.W., Huh H., 2014, Modeling of shear ductile fracture considering a changeable cut-off value for stress triaxiality, *International Journal of Plasticity* **54**: 56-80.

[41] Sun X., Choi K.S., Liu W.N., Khaleel M.A., 2009, Predicting failure modes and ductility of dual phase steels using plastic strain localization, *International Journal of Plasticity* **25**: 1888-1909.

[42] Gruben G., Fagerholt E., Hopperstad O.S., Børvik T., 2011, Fracture characteristics of a cold-rolled dual-phase steel, *European Journal of Mechanics* **30**: 204-218.

[43] Chung K., Ma N., Park T., 2011, A modified damage model for advanced high strength steel sheets, *International Journal of Plasticity* **27**: 1485-1511.

[44] Huh H., Kim S-B., Song J-H., Lim J-H., 2008, Dynamic tensile characteristics of TRIP-type and DP-type steel sheets for an auto-body, *International Journal of Mechanical Sciences* **50**: 918-931.

[45] Curtze S., Kuokkala V-T., Hokka M., Peura P., 2009, Deformation behavior of TRIP and DP steels in tension at different temperatures over a wide range of strain rates, *Materials Science and Engineering* **507**: 124-131.

[46] Roth C.C., Mohr D., 2014, Effect of strain rate on ductile fracture initiation in advanced high strength steel sheets: Experiments and modeling, *International Journal of Plasticity* **56**: 19-44.

[47] Mirfalah S.M., Basti A., Hashemi R., 2016, Forming limit curves analysis of aluminum alloy considering the through-thickness normal stress, anisotropic yield functions and strain rate, *International Journal of Mechanical Sciences* **117**: 93-101.

[48] Jie M., Cheng C.H., Chan L.C., Chow C.L., 2009, Forming limit diagrams of strain-rate-dependent sheet metals, *International Journal of Mechanical Sciences* **51**: 269-275.

[49] Saradar M., Basti A., Zaeimi M., 2015, Numerical study of the effect of strain rate on damage prediction by dynamic forming limit diagram in high velocity sheet metal forming, *Modares Mechanical Engineering* **14**: 212-222.

[50] Wu H-Y., Sun P-H., Chen H-W., Chiu C-H., 2012, Rate and orientation dependence of formability in fine-grained AZ31B-O Mg alloy thin sheet, *Journal of Materials Engineering and Performance* **21**: 2124-2130.

[51] Kim D., Kim H., Kim J.H., 2015, Modeling of forming limit for multilayer sheets based on strain-rate potentials, *International Journal of Plasticity* **75**: 63-99.

[52] Fakir O. El., Wang L., Balint D., 2014, Predicting effect of temperature, strain rate and strain path changes on forming limit of lightweight sheet metal alloys, *Procedia Engineering* **81**: 736-741.